NeuroImage: Clinical 26 (2020) 102196

Contents lists available at ScienceDirect

NeuroImage: Clinical

journal homepage: www.elsevier.com/locate/ynicl

Topography of cortical thinning in the Lewy body diseases

Rong Ye[a,1], Alexandra Touroutoglou[a,b,1], Michael Brickhouse[a,b], Samantha Katz[c], John H. Growdon[a], Keith A. Johnson[a,b,c], Bradford C. Dickerson[a,b], Stephen N. Gomperts[a,*]

[a] Department of Neurology, Massachusetts General Hospital, Charlestown, MA, USA
[b] Athinoula A. Martinos Center for Biomedical Imaging, Massachusetts General Hospital, Charlestown, MA, USA
[c] Department of Radiology, Massachusetts General Hospital, Boston, MA, USA

ARTICLE INFO

Keywords:
Cortical thinning
Amyloid deposition
Dementia with lewy bodies
Parkinson disease

ABSTRACT

Objective: Regional cortical thinning in dementia with Lewy bodies (DLB) and Parkinson disease dementia (PDD) may underlie some aspect of their clinical impairments; cortical atrophy likely reflects extensive Lewy body pathology with alpha-synuclein deposits, as well as associated Alzheimer's disease co-pathologies, when present. Here we investigated the topographic distribution of cortical thinning in these Lewy body diseases compared to cognitively normal PD and healthy non-PD control subjects, explored the association of regional thinning with clinical features and evaluated the impact of amyloid deposition.

Methods: Twenty-one participants with dementia with Lewy bodies (DLB), 16 with Parkinson disease (PD) - associated cognitive impairment (PD-MCI and PDD), and 24 cognitively normal participants with PD underwent MRI, PiB PET, and clinical evaluation. Cortical thickness across the brain and in regions of interest (ROIs) was compared across diagnostic groups and across subgroups stratified by amyloid status, and was related to clinical and cognitive measures.

Results: DLB and PD-impaired groups shared a similar distribution of cortical thinning that included regions characteristic of AD, as well as the fusiform, precentral, and paracentral gyri. Elevated PiB retention in DLB and PD-impaired but not in PD-normal participants was associated with more extensive and severe cortical thinning, in an overlapping topography that selectively affected the medial temporal lobe in DLB participants. In DLB, greater thinning in AD signature and fusiform regions was associated with greater cognitive impairment.

Conclusions: The pattern of cortical thinning is similar in DLB and PD-associated cognitive impairment, overlapping with and extending beyond AD signature regions to involve fusiform, precentral, and paracentral regions. Cortical thinning in AD signature and fusiform regions in these diseases reflects cognitive impairment and is markedly accentuated by amyloid co-pathology. Further work will be required to determine whether the distinct topography of cortical thinning in DLB and PD-associated cognitive impairment might have value as a diagnostic and/ or outcome biomarker in clinical trials.

1. Introduction

The Lewy body diseases—dementia with Lewy bodies (DLB), Parkinson disease dementia (PDD), and Parkinson disease (PD)—are characterized neuropathologically by neuronal inclusions of α-synuclein in cortical and subcortical regions as well as loss of neuromodulator neuronal populations including dopamine cells of the substantia nigra pars compacta and cholinergic cells of the basal forebrain (Gomperts, 2014; Halliday et al., 2014). The shared clinical features of DLB and PDD—which together comprise the Lewy body dementias (LBD)—include progressive cognitive impairment in association with parkinsonism, visual hallucinations, rapid eye movement sleep behavior disorder (RBD), and fluctuations in alertness and cognition. This clinical overlap suggests that the common neuropathology of the LBD impacts an overlapping set of vulnerable brain regions.

Imaging-based assessments of regional cortical atrophy in the LBD have provided a valuable approach to detect affected cortical regions (Song et al., 2011; Summerfield et al., 2005; Watson et al., 2015;

Abbreviations: CDR-SB, Clinical Dementia Rating Sum of Box; DLB, Dementia with Lewy bodies; H & Y, Hoehn and Yahr scale; MMSE, Mini-Mental State Examination; HC, healthy controls; PD, Parkinson disease; PiB, Pittsburgh compound B; UPDRS, Unified Parkinson Disease Rating Scale

* Corresponding author at: Department of Neurology, Building 114, 16th Street - 2004, Charlestown, MA, 02129-4404.
E-mail address: sgomperts@partners.org (S.N. Gomperts).

[1] R.Y. and A.T. contributed equally to this work.

https://doi.org/10.1016/j.nicl.2020.102196
Received 17 September 2019; Received in revised form 21 January 2020; Accepted 22 January 2020
Available online 31 January 2020

Weintraub et al., 2011). Although atrophy has been reported in both diseases, cortical volume loss is often more extensive and severe in DLB than PDD (Beyer et al., 2007; Borroni et al., 2015; Burton et al., 2004; Lee et al., 2010; Sanchez-Castaneda et al., 2009). One contributor to this distinction may be the greater prevalence and severity of concomitant Alzheimer's disease (AD)-related pathologic changes in DLB, including amyloid plaques and neurofibrillary tangles observed at autopsy (Harding and Halliday, 2001). Indeed, the presence of amyloid deposition in DLB (Gomperts, 2014) has been associated with greater cortical thinning (Lee et al., 2018; Mak et al., 2019), greater medial temporal atrophy (van der Zande et al., 2018), and a faster rate of cortical atrophy (Sarro et al., 2016). Studies aggregating patients with DLB, PDD, and the Lewy body variant of AD concur: cortical thinning was greater in the presence of amyloid and extended into widespread association cortices (Kang et al., 2019; Shimada et al., 2013). However, to our knowledge, the impact of amyloid on cortical thinning in PD and PDD has not been directly assessed.

In AD, a stereotyped topography of cortical thinning has been replicated in multiple studies; known as the “AD signature,” this distributed pattern of cortical atrophy involves heteromodal and paralimbic cortical regions known to be affected by AD neuropathology (Bakkour et al., 2009, 2013; Dickerson et al., 2009, 2011; Racine et al., 2018). In DLB, concomitant amyloid deposition evident on amyloid PET appears to drive a pattern of cortical thinning similar to AD, with additional regional thinning that may reflect the underlying synucleinopathy (Lee et al., 2018). To assess whether these observations extend to PDD and to explore how regional cortical thinning relates to clinical features of the Lewy body diseases, here we compared MR measures of cortical thinning in DLB, cognitively impaired PD and cognitively normal PD, assessed the impact of amyloid burden on the topography and severity of cortical thinning, and related regional cortical thinning to clinical features. We hypothesized that the topography of cortical thinning would be similar in DLB and cognitively impaired PD, overlapping with the “AD signature” on the basis of amyloid accumulation, with additional cortical involvement relevant to the distinguishing clinical features of the LBD. We also predicted that cortical amyloid would increase thinning in both groups, and that regional thinning in DLB and PD would relate to cognitive and motor impairments.

2. Methods

2.1. Participants and clinical assessments

Twenty-one participants with DLB, 16 PD with a broad range of cognitive impairments (PD-impaired; including 7 with PD-MCI and 9 with PDD), and 24 cognitively-normal individuals with PD (PD-normal) were recruited from Massachusetts General Hospital's Movement and Memory Disorder Units. All participants with DLB fulfilled the consortium criteria for probable DLB (McKeith et al., 2017). Participants with PD met the clinical criteria of the UK Parkinson's Disease Society Brain Bank (Hughes et al., 1993). Subjects with PD-MCI met level II Movement Disorder Society (MDS) Task Force guidelines (Litvan et al., 2012). The clinical MDS criteria for probable PDD were used for diagnosis of PDD participants (Emre et al., 2007). Subjects underwent clinical evaluation including scoring of motor function with the Unified Parkinson Disease Rating Scale part III (UPDRS-III) and detailed neuropsychological tests of the Unified Data Set of the Alzheimer's Disease Research Centers (Beekly et al., 2007; Morris et al., 2006), including the Clinical Dementia Rating Sum-of-Boxes score (CDR-SB), Mini-Mental State Examination (MMSE), Neuropsychiatric Inventory Questionnaire for assessment of hallucinations, and Mayo fluctuations scale (Ferman et al., 2004). The diagnostic groups were well matched for age (Table 1). Across all participants, the extent of concomitant small vessel disease evident on MR imaging was either absent or mild. Subjects with significant white matter hyperintensities (WMH), defined as either confluent deep WMH or irregular periventricular WMH extending into the deep white matter, were excluded. Thirty-one subjects underwent dopamine transporter PET imaging for purposes unrelated to the current study; putamen DAT concentration was reduced in all. The diagnosis of Lewy body disease was confirmed with neuropathological evaluation in all 18 cases that came to autopsy.

MR data from 115 age-matched healthy cognitively normal (CDR 0) individuals acquired in previous studies (Bickart et al., 2014; Dickerson et al., 2009; Moriguchi et al., 2011) were also employed for vertex-based and regions of interest (ROIs) - based cortical thickness analyses.

This study was approved by the Partners Human Research Committee Institutional Review Board of Partners Healthcare, Inc.

2.2. Neuroimaging procedures

Patient were scanned in an identical manner on a 3T Tim Trio (Siemens). High resolution structural T1-weighted magnetization-prepared rapid gradient-echo (MPRAGE) sequence were acquired with the following parameters: (TR = 2.3 ms, TE = 2.98 ms, flip angle = 9°, field of view = 240 mm × 256 mm, slice thickness = 1 mm and TR = 2.53 ms, TE = 1.64 ms, flip angle = 7°, field of view = 256 mm × 256 mm, slice thickness = 1 mm) processed with Freesurfer (version 6.0, freely available at http://surfer.nmr.mgh.harvard.edu). For all subjects, procedures for data collection included head movement restriction using expandable foam cushions, and automated scout and shimming procedures.

The technical details for MRI morphometric data analysis have been previously described in detail (Fischl and Dale, 2000; Fischl et al., 1999; Salat et al., 2004). In brief, for each individual subject, cortical thickness at each surface location (vertex) was measured as the average of the closest distance from the gray matter/white matter boundary to the corresponding cortical surface. The accuracy for this measurement has been validated by direct comparisons with manual measures on post-mortem brain (Rosas et al., 2002) and on MRI data (Kuperberg et al., 2003). After visual inspection for each individual subject, the cortical thickness data were smoothed along the cortical surface using a Gaussian kernel with a full width at half maximum of 15 mm.

Based on study hypotheses, we obtained cortical thickness from AD signature regions of cortical thinning (Bakkour et al., 2009; Dickerson et al., 2009). The AD signature ROIs were selected on the basis of their relevance to cognitive function and anticipated vulnerability to cortical amyloid. Cortical thickness values from these ROIs were then subjected to statistical analyses for ROIs as described below (Sections 2.3).

In addition, we obtained cortical thickness from three ROIs of the Desikan-Killiany atlas (Desikan et al., 2006) determined based on the exploratory vertex-based analysis of the statistical surface maps for the contrast of DLB vs. HC groups. These ROIs which included precentral, paracentral, and fusiform regions were anticipated to relate to clinical features in the Lewy body diseases. Cortical thickness values from these ROIs were subjected to statistical analyses for ROIs as described below (Sections 2.3). To generate the statistical surface maps, we computed a two-class general linear model for the effects of diagnostic group on cortical thickness at each point (threshold $P < 0.05$, FDR corrected).

[11C]PiB PET was acquired using a Siemens/CTI (Knoxville, TN) ECAT HR+ scanner (63 image planes; 15.2 cm axial field of view; 4.1 mm transaxial resolution and 2.4 mm slice interval) with a 8.5 to 15 mCi bolus injection followed immediately by a 60-minute dynamic acquisition in 39 frames (8 × 15 s, 4 × 60 s, 27 × 120 s). PET data were reconstructed and attenuation corrected, and each frame was evaluated to verify adequate count statistics and absence of head motion. [11C]PiB PET data were expressed as the distribution volume ratio (DVR) with cerebellar gray as reference. [11C]PiB retention was assessed using a large cortical ROI aggregate comprised of frontal, lateral temporal and retrosplenial cortices (FLR). For use as a dichotomous measure, high Aβ was defined as FLR DVR ≥ 1.32 after partial volume

Table 1
Demographic and clinical characteristics of participants.

Group	N	Sex (M/F)	Age (years)	Education (years)	Duration of Motor Impairment (years) [a, b]	Duration of Cognitive Impairment (years)	MMSE [a, b]	CDR-SB [a, b]	UPDRS-III [a]	H & Y	Hallucination [a] (N,%)
DLB	21	18/3	71.6 (7.1)	15.9 (2.6)	3.3 (1.4) [c, d]	4.8 (2.3)	20.4 (8.4) [c, d]	7.2 (5.0) [c, d]	30.9 (14.1) [d]	2.4 (0.9)	11 (52.4) [d]
Aβ $^{+}$	10	8/2	74.1 (4.1)	16.1 (2.9)	3.2 (1.4) [f]	5.3 (3.0)	17.6 (10.3) [f, g]	8.1 (5.3) [f, g]	27.5 (17.7)	2.2 (1.2)	5 (50.0)
Aβ $^{-}$	9	8/1	70.1 (9.0)	15.9 (2.6)	3.3 (1.7) [h, i]	4.2 (1.6)	23.4 (4.4) [i]	5.8 (4.0) [i, j]	31.6 (7.9)	2.4 (0.5)	5 (55.6)
PD-impaired	16	12/4	73.1 (7.2)	16.7 (2.4)	9.4 (4.7) [c]	4.4 (3.2)	24.9 (3.3) [c, e]	3.3 (2.6) [c, e]	28.0 (10.7)	2.7 (0.8)	5 (31.3) [e]
Aβ $^{+}$	7	5/2	71.6 (7.2)	16.4 (2.3)	8.4 (2.9)	4.9 (2.1)	23.3 (3.7) [k]	4.1 (3.2)	29.0 (12.4)	2.7 (0.7)	3 (42.9)
Aβ $^{-}$	9	7/2	74.2 (7.3)	16.9 (2.7)	10.2 (5.8) [f, h]	4.1 (3.9)	26.1 (2.4) [f]	2.6 (2.0) [f]	27.2 (9.8)	2.7 (0.8)	2 (22.2)
PD-normal	24	16/8	69.0 (6.9)	16.7 (2.9)	9.3 (5.4) [d]	–	29.6 (0.6) [d, e]	0.2 (0.3) [d, c]	19.8 (10.9) [d]	2.3 (0.8)	1 (4.2) d, [e]
Aβ $^{+}$	6	5/1	73.1 (6.8)	17.7 (2.0)	5.3 (2.3)	–	29.3 (0.8) [g]	0.1 (0.2) [g, j]	17.0 (9.3)	2.2 (0.3)	0 (0)
Aβ $^{-}$	18	11/7	67.6 (6.5)	16.4 (3.1)	10.6 (5.5) [f, i]	–	29.7 (0.5) [f, i, k]	0.2 (0.3) [f, i]	20.8 (11.5)	2.3 (0.9)	1 (5.6)
HC	115	–	69.4 (7.4)	–	–	–	–	–	–	–	–

Abbreviations: CDR-SB, Clinical Dementia Rating Sum of Box; DLB, Dementia with Lewy bodies; H & Y, Hoehn and Yahr stage; MMSE, Mini-Mental State Examination; HC, healthy controls; PD, Parkinson disease; PiB, Pittsburgh compound B; UPDRS, Unified Parkinson Disease Rating Scale.
Values represent mean (standard deviation) unless otherwise noted. Group analyses were tested among DLB, PD-impaired, and PD-normal groups. Subgroup differences were tested among amyloid positive and negative DLB, PD-impaired and PD-normal groups. Average ages of all groups, subgroups and HC were similar. Note that amyloid status of two DLB participants was unknown; they were not included in subsequent subgroup analyses.

[a] Between group difference, $p < 0.05$, ANOVA; for analysis of hallucination, $p < 0.05$, Chi square test.
[b] Between subgroup difference, $p < 0.05$, ANOVA.
[c] DLB vs. PD-impaired, $p < 0.05$, Tukey's post hoc test.
[d] DLB vs. PD-normal, $p < 0.05$, Tukey's post hoc test; for analysis of hallucination, $p < 0.05$, Chi square test.
[e] PD-impaired vs. PD-normal, $p < 0.05$, Tukey's post hoc test; for analysis of hallucination, $p < 0.05$, Chi square test.
[f] Amyloid-positive DLB vs. amyloid-negative PD-impaired, amyloid-positive DLB vs. amyloid-negative PD-normal, $p < 0.05$, Tukey's post hoc test.
[g] Amyloid-positive DLB vs. amyloid-positive PD-normal, $p < 0.05$, Tukey's post hoc test.
[h] Amyloid-negative DLB vs. amyloid-negative PD-impaired, $p < 0.05$, Tukey's post hoc test.
[i] amyloid-negative DLB vs. amyloid-negative PD-normal, $p < 0.05$, Tukey's post hoc test.
[j] amyloid-negative DLB vs. amyloid-positive PD-normal, $p < 0.05$, Tukey's post hoc test.
[k] amyloid-positive PD-impaired vs. amyloid-negative PD-normal, $p < 0.05$, Tukey's post hoc test.

correction using SGTM (Greve et al., 2016), based on a Gaussian mixture model on a reference dataset of clinically normal elderly (Mormino et al., 2014). In three participants, amyloid status was made either via visual assessment (PiB negative, $n = 1$ DLB) or autopsy (Aβ negative, A1B1C1, $n = 1$ DLB; Aβ positive, A3B2C2, $n = 1$ PDD) (Hyman et al., 2012). Two DLB subjects lacked [11C]PiB scans or autopsy results and were excluded from amyloid subgroup analyses.

To examine the effect of amyloid deposition on cortical thinning in LBD, we stratified DLB and PD-impaired subjects by amyloid status (+/-). In vertex-based analysis, we generated statistical surface maps by computing a two-class general linear model comparing healthy controls with amyloid-positive DLB, amyloid-negative DLB, amyloid-positive PD-impaired and amyloid-negative PD-impaired groups. In ROIs analysis, the AD signature regions and the three additional ROIS (fusiform, precentral and paracentral) were subjected to statistical analyses as described below (Sections 2.3).

2.3. Statistical analysis

Group statistical comparisons were performed using analysis of variance with post hoc pairwise comparisons for continuous measures or χ^2 for proportions. In ROI analyses, Bonferroni correction was used for comparisons across multiple ROIs. Relationships between continuous measures (e.g., between regional anatomic measures and the severity of clinical symptoms) were assessed with Spearman correlations, adjusting for age. Statistical analyses were conducted using R Software (version 3.3.3, freely available at https://www.r-project.org/).

3. Results

3.1. Clinical characteristics

Participant characteristics are presented in Table 1. The DLB, PD-impaired and PD-normal groups did not differ on the basis of age, years of education, or sex, which was skewed toward men in all disease groups. Cognitive impairment measured with MMSE and CDR-SB scores was greater in DLB than in the PD-impaired group (for each contrast, Tukey's post hoc t-test, $p < 0.05$). Motor impairments assessed with the UPDRS motor subscale and Hoehn and Yahr (H&Y) stage were similar in DLB and PD-impaired groups. However, the severity of motor impairments on UPDRS was greater in DLB than in the PD-normal group (ANOVA, $F(2, 58) = 5.1$, $p = 0.01$; Tukey's post hoc t-test, $p = 0.01$). Visual hallucinations were common in DLB (prevalence 52.4%) and PD-impaired subjects (prevalence 31.3%) but were rare in PD-normal subjects (prevalence 4.2%; contrast of DLB vs. PD-normal, $\chi^2 = 13.3$, $p < 0.001$; contrast of PD-impaired vs PD-normal, $\chi^2 = 5.5$, $p = 0.02$).

When DLB and PD-impaired subjects were stratified by amyloid status (+/-), age, sex, and years of education were comparable across the four subgroups. Amyloid deposition was common in both DLB (fraction amyloid positive: 10/19) and PD-impaired subjects (7/16). The extent of deposition was similar in DLB compared to PD-impaired subjects (FLR DVR, DLB 1.68 ± 0.58, PD-impaired 1.30 ± 0.22, Mann-Whitney test, $p = 0.11$). In the PD-normal group, 6/24 had elevated PiB retention. Amyloid status did not impact cognitive impairment within diagnostic groups. Motor impairments and the prevalence of visual hallucinations were similar across all subgroups.

3.2. Patterns of cortical thinning

In DLB, vertex-based analyses demonstrated widespread cortical thinning ($p < 0.05$, FDR corrected), most severe in frontal, parietal, lateral and medial temporal regions (Fig. 1A). In the PD-impaired group, thinning was evident in an overlapping distribution ($p < 0.05$, FDR corrected) but spared medial temporal regions (Fig. 1B). The distribution of cortical thinning in the DLB and PD-impaired groups included AD signature regions (nine cortical ROIs), with additional involvement of precentral, paracentral, and fusiform regions (Fig. 2A; Table 2; Supplementary Table 1). No significant cortical thinning was observed in the PD-normal group.

Similar results were observed at the ROI level: both DLB and PD-impaired groups had marked cortical thinning in the AD signature regions taken as a whole, compared to PD-normal and HC groups (Fig. 2B, ANOVA, $F(3, 172) = 23.2$, $p = 1 \times 10^{-12}$; Tukey's post hoc t-test, $p < 0.005$). Compared to PD-normal and HC groups, both DLB and PD-impaired groups showed significant thinning in primary motor (aggregated precentral and paracentral) regions (Fig. 2C, ANOVA, $F(3, 172) = 14.1$, $p = 3 \times 10^{-8}$; Tukey's post hoc t-test, $p < 0.05$), as well as in the fusiform (Fig. 2D, ANOVA, $F(3, 172) = 22.3$, $p = 3 \times 10^{-12}$; Tukey's post hoc t-test, $p < 0.05$). No significant difference was observed in the extent of cortical thinning between DLB and PD-impaired groups in the AD signature, primary motor, or fusiform regions.

Cortical thinning in DLB was greatest in the medial temporal cortex with a mean magnitude of thinning of 0.39 mm (12% reduction compared to HC, ANOVA, $F(3, 172) = 9.5$, $p = 8 \times 10^{-6}$; Tukey's post hoc t-test, $p = 6 \times 10^{-5}$, Bonferroni corrected for number of ROIs). Other regions with more than 0.2 mm thinning included the precentral, fusiform, temporal pole, and inferior parietal (supramarginal) regions, which ranged from 8.8 – 10.5% thinner than HC (each comparison, Tukey's post hoc t-test, $p < 0.001$, Bonferroni corrected). A smaller magnitude of thinning (0.13–0.19 mm, 5.8–7.6%) was also observed in inferior temporal, precuneus, angular, paracentral, inferior frontal, superior frontal and superior parietal regions (Tukey's post hoc t-test, $p < 0.05$, Bonferroni corrected).

In the PD-impaired group, in contrast to DLB, cortical thickness in medial and inferior temporal regions was normal (ANOVA, for medial temporal cortex, $F(3, 172) = 9.5$, $p = 8 \times 10^{-6}$, for inferior temporal cortex, $F(3, 172) = 7.1$, $p = 2 \times 10^{-4}$; Tukey's post hoc t-test, for medial temporal cortex, $p = 0.36$, for inferior temporal cortex, $p = 0.09$). Cortical thinning in PD-impaired subjects was greatest in superior frontal cortex (0.22 mm, 8.4% reduction, ANOVA, $F(3, 172) = 12.9$, $p = 1 \times 10^{-7}$; Tukey's post hoc t-test, $p = 2 \times 10^{-4}$, Bonferroni corrected). Cortical thinning was also observed in the precentral (0.20 mm, 8.1%) and paracentral cortex (0.14 mm, 5.9%), fusiform (0.12 mm, 4.6%), precuneus (0.18 mm, 7.2%), superior parietal lobule (0.16 mm, 7.3%), and angular gyrus (0.15 mm, 6.2%) (all contrasts, Tukey's post hoc t-test, $p < 0.05$, Bonferroni corrected). The severity of cortical thinning was similar in the PD-impaired group and the DLB group in each of these regions, except for fusiform cortical thickness which was thinner in DLB compared to the PD-impaired group but did not survive multiple comparisons correction (ANOVA, $F(3, 172) = 22.3$, $p = 3 \times 10^{-12}$; Tukey's post hoc t-test, $p = 0.04$, Bonferroni uncorrected). As mentioned previously, the fusiform gyrus is not a consistent area of cortical thinning in AD. Interestingly, the three other areas with the most prominent thinning in DLB (medial temporal cortex, temporal pole, and supramarginal gyrus) are also consistently affected in AD and were much less affected in the PD-impaired group. Of note, when analyses were restricted to subjects with PDD, cortical thickness in the medial temporal cortex remained similar to HC (ANOVA, $F(3, 165) = 9.7$, $p = 6 \times 10^{-6}$; Tukey's post hoc t-test, $p = 0.42$).

Together, these results show that the DLB and PD-impaired groups shared a largely similar spatial pattern of cortical thinning that extended beyond the AD signature regions but differed with respect to temporal lobe involvement, with the DLB group having much more widespread medial, ventral, and ventrolateral temporal cortex thinning than the PD-impaired group.

3.3. The effect of amyloid accumulation on cortical thinning in LBD

In vertex-based analyses, DLB and PD-impaired subjects with high PiB retention (amyloid positive) showed more extensive and severe

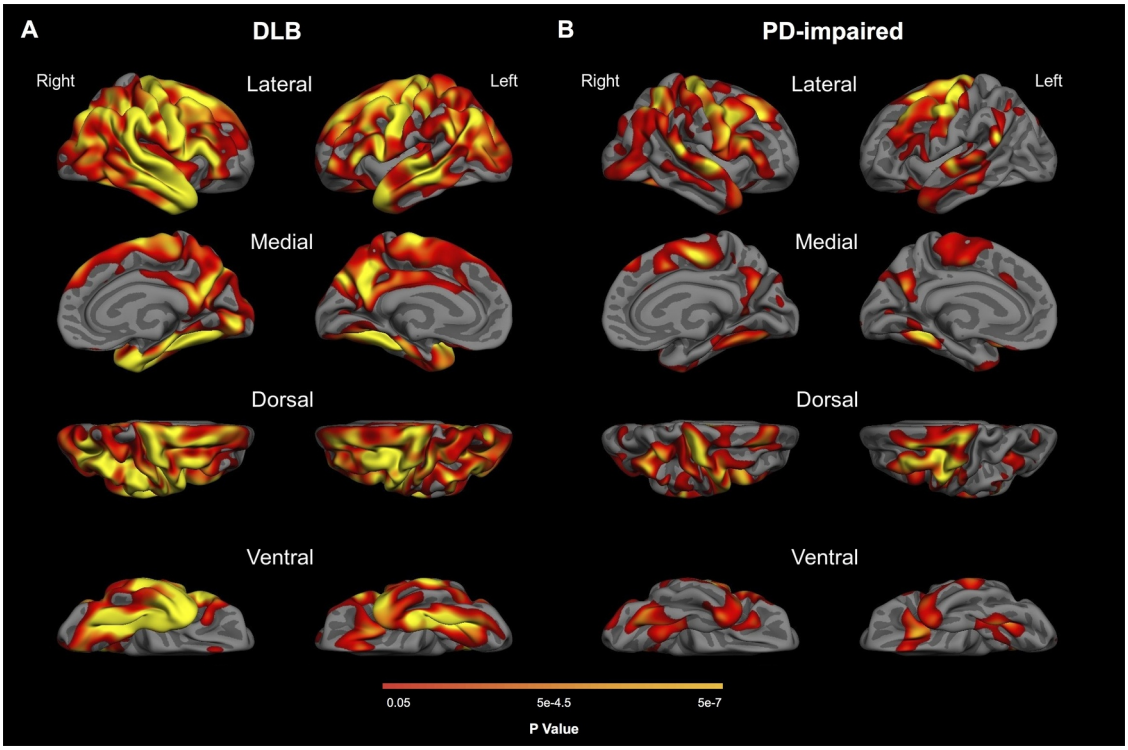

Fig. 1. Patterns of cortical thinning in DLB and PD-impaired groups. Maps show FDR-corrected ($p < 0.05$) results from general linear models comparing healthy controls with (A) DLB and (B) PD-impaired groups.

cortical thinning than subjects with low PiB retention (amyloid negative) (Fig. 3). The topography and extent of cortical thinning was broadly similar in amyloid-positive DLB and PD-impaired subjects, evident in both groups in frontal, parietal, and lateral temporal regions including AD-signature regions. However, as in the above analyses, the medial, ventral, and lateral temporal lobes showed a notably more widespread pattern of cortical thinning in amyloid-positive DLB than in the amyloid-positive PD-impaired group. In the amyloid-positive PD-impaired group, a relatively more prominent pattern of thinning in the dorsolateral prefrontal cortex was present, compared with DLB. The medial temporal cortex was spared in the PD-impaired group. In contrast, the pattern of cortical thinning evident in amyloid-negative DLB was much more restricted, with effects in dorsolateral prefrontal, precentral, and temporal cortex, but with much less lateral or medial parietal atrophy than in both amyloid-positive groups. Cortical thinning was not detected in amyloid-negative PD-impaired subjects. We were unable to detect an effect of amyloid deposition on cortical thickness in PD-normal patients in either vertex-based or ROI analyses. To confirm that the nonsignificant differences in age between groups did not contribute to these results or to the group contrasts independent of amyloid, we reran the analyses, contrasting the diagnostic groups with healthy control subjects tightly matched for age. After matching for mean and median age, the gamma maps remained essentially unchanged.

ROI-based analyses confirmed the vertex-based results. In ROI-based analyses of amyloid-positive DLB, the medial temporal lobe was most affected (0.44 mm, 13% thinning compared to HC), followed by the fusiform (0.36 mm, 13%), with additional cortical thinning in precentral, precuneus, supramarginal, angular, inferior frontal, and temporal polar regions (for each comparison: Tukey's post hoc test, $p < 0.05$, Bonferroni corrected for the number of ROIs; Table 3). In the amyloid-negative DLB subgroup, cortical thinning was less marked than in the amyloid-positive DLB subgroup. Interestingly, all but one ROI (the superior frontal gyrus) were slightly though not statistically thinner in the amyloid-positive DLB group than in the entire DLB group, whereas all but that same ROI were slightly though not statistically thicker in the amyloid-negative DLB group than in the entire DLB group. Considered with the more widespread spatial pattern of cortical thinning illustrated in the surface maps (Fig. 3), this suggests that cerebral amyloid is associated with greater cortical thinning in DLB. In ROI-based analyses of the amyloid-positive PD-impaired subgroup, the precentral region showed the greatest thinning (0.30 mm, 12% thinning), followed by the precuneus (0.21 mm, 12% thinning), with additional cortical thinning in superior frontal, paracentral, and angular regions (for each comparison: Tukey's post hoc test, $p < 0.05$, Bonferroni corrected). Cortical thinning was not evident at the ROI level in amyloid-negative PD-impaired subjects. Thus, in DLB and PD-impaired subjects but not in PD-normal subjects, amyloid deposition was associated with greater cortical thinning.

3.4. Regional cortical thinning relates to clinical features

In the DLB group, cortical thickness in the AD signature was negatively correlated with cognitive functional impairment as measured with the CDR-SB score (age adjusted partial Spearman rho $= -0.52$, $p = 0.02$) and was positively correlated with the MMSE score (partial Spearman rho $= 0.48$, $p = 0.03$; Fig. 4A,B). In the PD-impaired group, these findings were not observed (CDR-SB: partial Spearman rho $= -0.13$, $p = 0.65$), although a trend level correlation of moderate strength was observed between AD signature cortical thickness and the MMSE (partial Spearman rho $= 0.46$, $p = 0.09$). When the analyses were restricted to subjects with PDD, these correlations remained nonsignificant (CDR-SB: partial Spearman rho $= -0.41$, $p = 0.31$; MMSE: partial Spearman rho $= 0.17$, $p = 0.68$). In the PD-normal group, correlations between AD signature cortical thickness and CDR-SB and MMSE score were nonsignificant (CDR-SB: partial Spearman rho $= -0.04$, $p = 0.87$; MMSE: partial Spearman rho $= 0.15$, $p = 0.49$). When the correlations between cortical thinning in the AD signature and these cognitive functional measures were repeated in diagnostic subgroups stratified by amyloid status, only a trend level

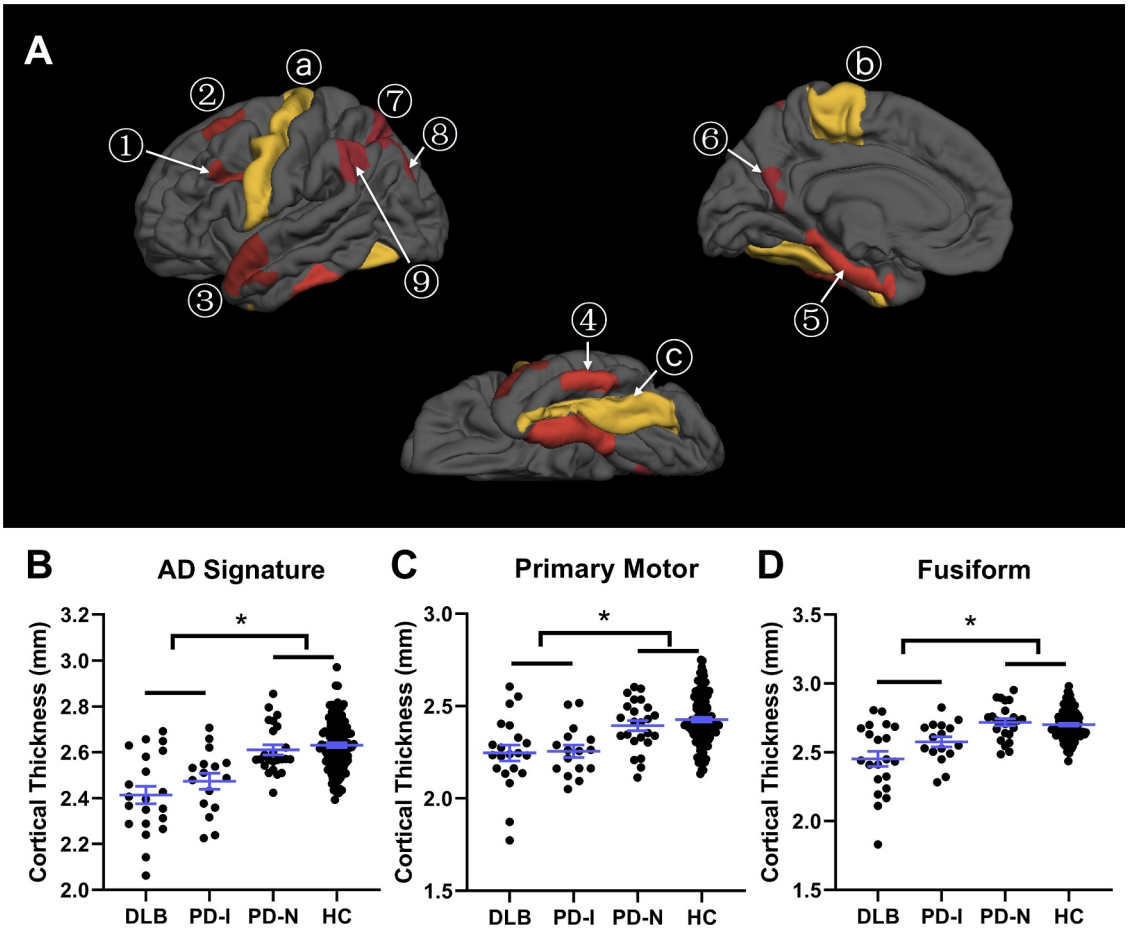

Fig. 2. Regional cortical thinning in LBD (A) Nine ROIs with characteristic thinning in AD derived from Dickerson et al. (2009) are shown in red, including ① inferior frontal sulcus, ② superior frontal gyrus, ③ temporal pole, ④ inferior temporal gyrus, ⑤ medial temporal cortex, ⑥ precuneus, ⑦ superior parietal lobule, ⑧ angular gyrus, and ⑨ supramarginal gyrus. Three additional regions, ⓐ precentral, ⓑ paracentral and ⓒ fusiform derived from the Desikan-Killiany atlas (Desikan et al., 2006) are shown in yellow. (B, C and D) Group comparisons of regional cortical thickness. Error bars (mean ± standard deviation) are displayed in blue. *, $p < 0.05$.

Table 2
Quantitative metrics of thinning by region .

ROIs	Mean thickness, mm (SD)				Mean difference			Percent thinning			Cohen d Effect Size		
	DLB	PD-I	PD-N	HC	DLB	PD-I	PD-N	DLB	PD-I	PD-N	DLB	PD-I	PD-N
MTL	2.96 (0.51)	3.21 (0.43)	3.36 (0.27)	3.35 (0.27)	0.39*	0.14	−0.01	11.68	4.21	0.29	1.24	0.49	0.04
IT	2.63 (0.27)	2.68 (0.24)	2.86 (0.16)	2.80 (0.19)	0.17*	0.12	−0.06	6.03	4.45	2.26	0.84	0.65	0.35
TP	2.67 (0.34)	2.77 (0.29)	3.02 (0.24)	2.98 (0.21)	0.31*	0.20 §	−0.05	10.53	6.86	1.54	1.34	0.94	0.22
AG	2.24 (0.19)	2.26 (0.15)	2.37 (0.15)	2.41 (0.15)	0.17*	0.15*	0.04	6.95	6.23	1.75	1.07	0.99	0.28
SFG	2.42 (0.25)	2.39 (0.19)	2.55 (0.18)	2.61 (0.15)	0.19*	0.22*	0.06	7.09	8.43	2.36	1.11	1.43	0.40
SPL	2.01 (0.17)	2.01 (0.19)	2.08 (0.14)	2.17 (0.15)	0.16*	0.16*	0.09	7.33	7.28	4.23	1.05	1.04	0.63
SMG	2.26 (0.22)	2.36 (0.15)	2.44 (0.19)	2.51 (0.17)	0.24*	0.15 §	0.06	9.72	5.80	2.58	1.36	0.87	0.37
Precuneus	2.35 (0.19)	2.36 (0.17)	2.55 (0.15)	2.54 (0.16)	0.19*	0.18*	−0.001	7.55	7.19	0.05	1.19	1.15	0.01
IFS	2.17 (0.13)	2.22 (0.10)	2.27 (0.14)	2.31 (0.12)	0.13*	0.09 §	0.04	5.79	3.79	1.85	1.11	0.75	0.35
FF	2.45 (0.25)	2.58 (0.15)	2.72 (0.13)	2.70 (0.11)	0.25*	0.12*	−0.02	9.18	4.62	0.66	1.78	1.10	0.16
PrC	2.26 (0.25)	2.28 (0.15)	2.43 (0.14)	2.48 (0.14)	0.22*	0.20*	0.04	8.82	8.12	1.76	1.40	1.48	0.32
ParC	2.23 (0.19)	2.24 (0.14)	2.36 (0.14)	2.38 (0.15)	0.14*	0.14*	0.02	5.99	5.90	0.88	0.92	0.96	0.14

Values represent mean (standard deviation) unless otherwise noted. For each ROI, average cortical thickness in disease groups was contrasted with healthy controls by ANOVA, following by Tukey's post hoc tests. Abbreviations: AG, Angular gyrus; DLB, Dementia with Lewy bodies; FF, Fusiform; IFS, Inferior frontal sulcus; IT, Inferior temporal gyrus; MTL, Medial temporal lobe; SFG, Superior frontal gyrus; SMG, Supramarginal gyrus; SPL, Superior parietal lobule; TP, Temporal pole; PD, Parkinson disease; PrC, Precentral; ParC, Paracentral.

* Disease group vs. healthy controls, $p < 0.05$, Bonferroni corrected for the number of ROIs.

§ Disease group vs. healthy controls, $p < 0.05$, uncorrected. These exploratory results did not survive after controlling for multiple comparisons.

correlation of moderate strength was observed for amyloid-negative DLB between AD signature thickness and CDR-SB score (for CDR-SB, amyloid-negative DLB: partial Spearman rho = −0.62, $p = 0.10$; amyloid-positive DLB: partial Spearman rho = −0.12, $p = 0.76$; amyloid-negative PD-impaired: partial Spearman rho = 0.25, $p = 0.55$; amyloid-positive PD-impaired: partial Spearman rho = −0.50, $p = 0.31$; for MMSE, amyloid-negative DLB: partial Spearman rho = 0.29, $p = 0.49$; amyloid-positive DLB: partial Spearman rho = 0.44, $p = 0.23$; amyloid-negative PD-impaired: partial Spearman rho = 0.33, $p = 0.43$; amyloid-positive PD-impaired: partial Spearman

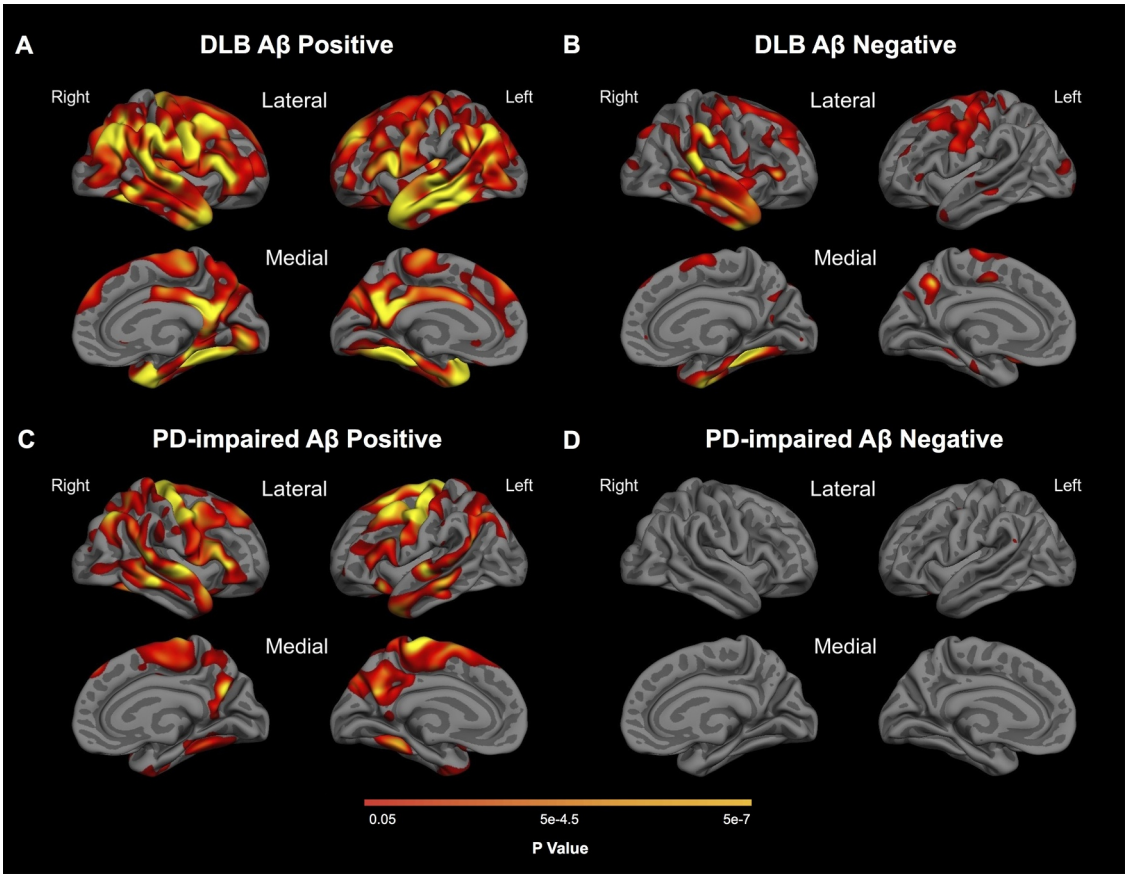

Fig. 3. Effect of amyloid deposition on cortical thinning in LBD. Maps show FDR-corrected ($p < 0.05$) results from general linear models comparing healthy controls with (A) amyloid-positive DLB, (B) amyloid-negative DLB, (C) amyloid-positive PD-impaired and (D) amyloid-negative PD-impaired groups.

rho = 0.36, $p = 0.49$).

Because the fusiform region has been implicated in higher order visual processing and expertise (Duchaine and Yovel, 2015), we next assessed whether fusiform cortical thickness also correlated with cognitive function. Similar to the above findings in AD-signature regions, fusiform cortical thickness correlated with cognitive impairment in DLB (CDR-SB score, age adjusted partial Spearman rho = −0.56, $p = 0.01$; MMSE score, partial Spearman rho = 0.57, $p = 0.01$; Fig. 4C,D). This correlation was not evident in the PD-impaired (CDR-SB score, partial Spearman rho = −0.28, $p = 0.30$; MMSE score, partial Spearman rho = 0.39, $p = 0.15$) or the PD-normal groups (CDR-SB score, partial Spearman rho = 0.11, $p = 0.63$; MMSE score, partial Spearman rho = −0.11, $p = 0.63$). Because visual hallucinations are common in the LBD, we also explored the possibility that fusiform cortical thickness might relate to the presence of visual hallucinations. However, DLB and PD-impaired diagnostic groups dichotomized on the basis of

Table 3
Quantitative metrics of thinning in subgroups stratified by amyloid status .

ROIs	Mean Thickness, mm (SD)				Mean difference				Percent thinning				Cohen d Effect Size			
	DLB		PD-impaired		DLB		PD-impaired		DLB		PD-impaired		DLB		PD-impaired	
Aβ Status	+	−	+	−	+	−	+	−	+	−	+	−	+	−	+	−
ADsig	2.38 (0.18)	2.43 (0.18)	2.41 (0.11)	2.53 (0.15)	0.25*	0.20*	0.22*	0.11	9.45	7.48	8.51	4.00	2.07	1.65	1.98	0.91
MTL	2.92 (0.67)	2.97 (0.37)	3.07 (0.42)	3.33 (0.43)	0.44*	0.39	0.29	0.03	13.06	11.52	8.53	0.86	1.39	1.40	1.03	0.10
IT	2.60 (0.18)	2.63 (0.33)	2.66 (0.21)	2.69 (0.26)	0.20	0.17	0.14	0.11	6.97	6.11	5.16	3.89	1.05	0.86	0.77	0.57
TP	2.61 (0.33)	2.70 (0.37)	2.70 (0.36)	2.83 (0.21)	0.37*	0.28	0.28	0.15	12.38	9.38	9.28	4.98	1.68	1.25	1.27	0.71
AG	2.18 (0.16)	2.28 (0.19)	2.17 (0.07)	2.33 (0.15)	0.23*	0.13	0.24*	0.08	9.53	5.35	10.05	3.27	1.70	0.92	1.17	0.62
SFG	2.46 (0.27)	2.37 (0.23)	2.34 (0.23)	2.43 (0.17)	0.15	0.24*	0.27*	0.18	5.70	9.26	10.25	7.01	0.93	1.56	1.75	1.22
SPL	2.00 (0.18)	2.02 (0.19)	1.95 (0.06)	2.06 (0.24)	0.17	0.15	0.21	0.11	7.87	6.80	9.91	5.24	1.14	0.98	1.50	0.73
SMG	2.21 (0.21)	2.35 (0.23)	2.31 (0.11)	2.40 (0.16)	0.29*	0.16	0.20	0.10	11.77	6.40	7.88	4.18	1.70	0.92	1.17	0.62
Precuneus	2.31 (0.17)	2.40 (0.22)	2.25 (0.14)	2.45 (0.15)	0.23*	0.15	0.21*	0.11	9.18	5.66	11.60	3.76	1.48	0.89	1.90	0.61
IFS	2.15 (0.09)	2.20 (0.16)	2.22 (0.09)	2.22 (0.11)	0.16*	0.11	0.09	0.08	6.82	4.83	3.94	3.68	1.34	0.91	0.77	0.72
FF	2.34 (0.26)	2.55 (0.22)	2.53 (0.15)	2.61 (0.14)	0.36*	0.15	0.17	0.09	13.18	5.68	6.30	3.31	2.83	1.29	1.54	0.81
PrC	2.25 (0.24)	2.28 (0.29)	2.18 (0.12)	2.35 (0.13)	0.23*	0.20*	0.30*	0.13	9.22	7.93	11.88	5.20	1.57	1.31	2.19	0.96
ParC	2.21 (0.15)	2.25 (0.25)	2.15 (0.06)	2.31 (0.15)	0.16	0.12	0.23*	0.07	10.19	8.03	4.04	4.98	1.10	0.79	1.58	0.48

Values represent mean (standard deviation) unless otherwise noted. For each ROI, average cortical thickness was contrasted in disease groups with healthy controls by ANOVA, following by Tukey's post hoc tests. Abbreviations: AG, Angular gyrus; DLB, Dementia with Lewy bodies; FF, Fusiform; IFS, Inferior frontal sulcus; IT, Inferior temporal gyrus; MTL, Medial temporal lobe; ParC, Paracentral; PrC, Precentral; PD, Parkinson disease; SFG, Superior frontal gyrus; SMG, Supramarginal gyrus; SPL, Superior parietal lobule; TP, Temporal pole.

* Disease group vs. healthy controls, $p < 0.05$, Bonferroni corrected for the number of ROIs.

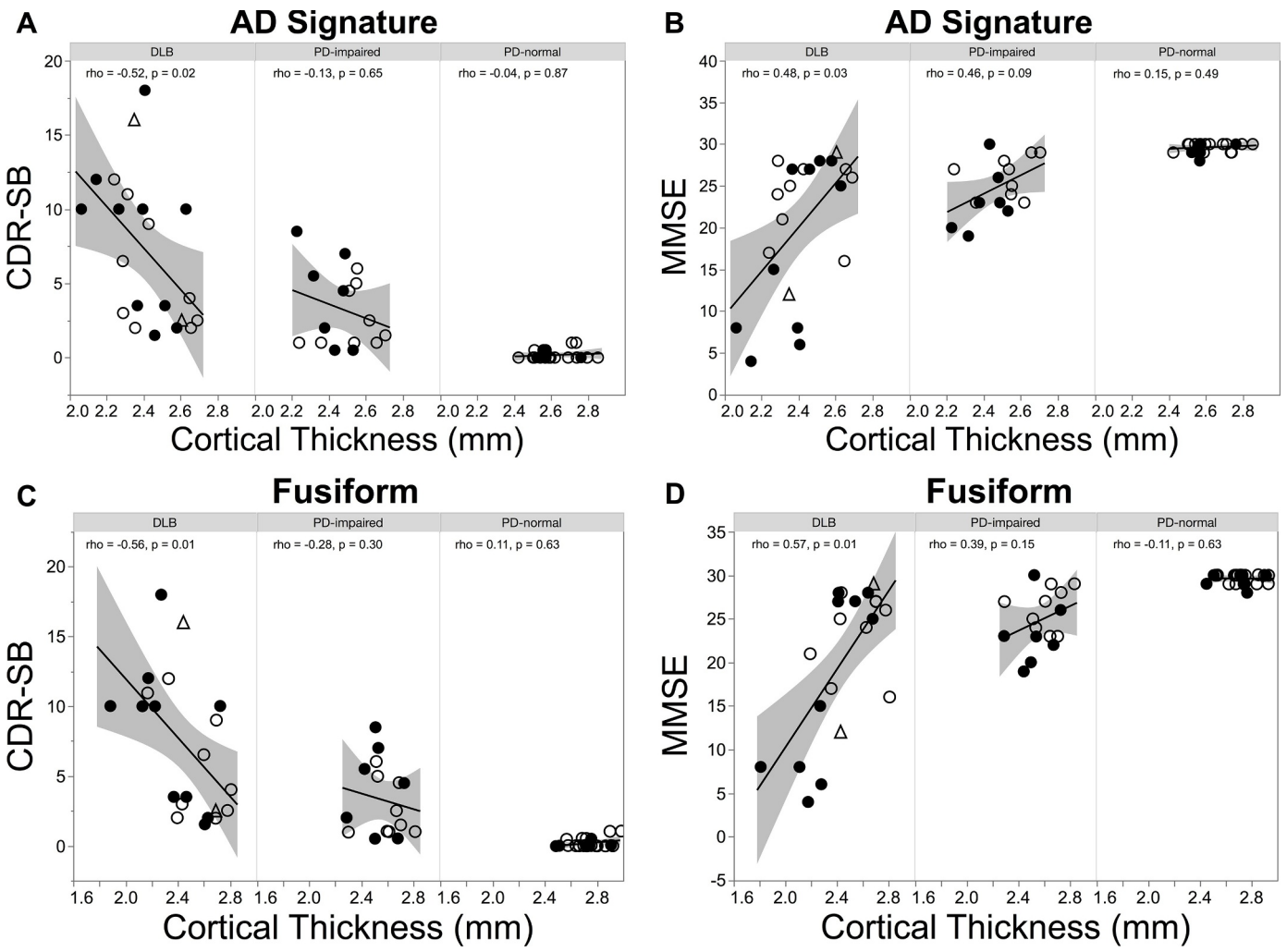

Fig. 4. Regional cortical thinning in LBD correlates with clinical features. Scatter plots between (A) AD signature cortical thickness and CDR-SB score, (B) AD signature cortical thickness and MMSE score, (C) fusiform cortical thickness and CDR-SB score, and (D) fusiform cortical thickness and MMSE score. Correlation coefficients rho and p values adjusted by age are shown. Filled circles, amyloid-positive status; open circles, amyloid-negative status; triangles, unknown amyloid status. .

visual hallucinations did not differ in their fusiform cortical thickness (DLB with hallucinations 2.44 ± 0.26, DLB without hallucinations 2.39 ± 0.30, two-tailed *t*-test, $p = 0.94$; PD-impaired with hallucinations 2.55 ± 0.16, PD-impaired without hallucinations 2.60 ± 0.15, two-tailed *t*-test, $p = 0.72$). These results persisted in contrasts of DLB and PD-impaired subgroups stratified by amyloid status: For both amyloid positive and amyloid negative diagnostic subgroups, the presence of hallucinations did not affect fusiform cortical thickness (for each diagnostic subgroup of each amyloid status, two-tailed *t*-test, $p > 0.51$).

Given that thinning in primary motor cortical regions was a prominent finding in DLB and PD-impaired groups, we next evaluated its relation to motor impairment. Within each diagnostic group, primary motor cortical thickness was not significantly correlated with UPDRS motor scores (DLB: partial Spearman rho $= -0.04$, $p = 0.86$; PD-impaired: rho $= -0.14$, $p = 0.62$; PD-normal: rho $= -0.21$, $p = 0.33$). To determine whether amyloid deposition impacted this relationship, we repeated these analyses after stratifying by amyloid status. In the amyloid-negative DLB subgroup alone, greater thinning in primary motor cortex was associated with greater impairment on the UPDRS (amyloid-negative DLB: partial Spearman rho $= -0.75$, $p = 0.03$; amyloid-positive DLB: partial Spearman rho $= 0.38$, $p = 0.32$; amyloid-negative PD-impaired: partial Spearman rho $= -0.27$, $p = 0.52$; amyloid-positive PD-impaired: partial Spearman rho $= 0.35$, $p = 0.50$; Supplemental Figure 1).

Together, these observations suggest that cortical thinning in AD signature and fusiform regions contributes to cognitive impairment in the LBD and raise the possibility that thinning in primary motor regions may contribute to motor impairment in DLB.

4. Discussion

The results of this study identify a pattern of cortical thinning shared between DLB and PD-impaired groups. The distribution of thinning overlapped with AD signature regions and extended to involve fusiform, precentral and paracentral cortex. In prior voxel-based morphometry studies, patterns of cortical atrophy in DLB and PDD have also been found to overlap (Burton et al., 2004), albeit with greater volume loss in DLB (Beyer et al., 2007; Sanchez-Castaneda et al., 2009; Song et al., 2011; Summerfield et al., 2005; Weintraub et al., 2011). Our results are also consistent with studies that have evaluated cortical thickness in DLB (Lee et al., 2018; Watson et al., 2015) and extend these findings to PD-associated cognitive impairment. The observation of thinning in primary motor cortices in the Lewy body diseases is interesting in light of the motor impairments that arise in these diseases. This finding is consistent with a neuropathological report showing that Lewy body pathology is associated with precentral cortical atrophy (Harper et al., 2017).

In DLB, amyloid deposition was associated with markedly accentuated thinning that was widely distributed across many cortical regions, including the medial temporal lobe, consistent with recent reports (Lee et al., 2018; Mak et al., 2019; van der Zande et al., 2018). In the absence of amyloid, cortical thinning in DLB could still be detected, revealing a synuclein-dependent pattern of cortical thinning that overlapped with and extended beyond the AD signature to include the precentral cortex, among other regions. However, medial temporal cortical thinning, a characteristic feature of AD, was much less prominent in DLB without amyloid than in DLB in the presence of cortical amyloid.

The impact of cortical amyloid in PD-impaired subjects was similar to DLB but distinct, driving distributed cortical thinning that spared the medial temporal cortex. The basis for this distinction is unclear but may relate to the nonsignificantly lower amyloid burden observed in the PD-impaired group compared to the DLB group. Differences between the groups in the level of cognitive impairment is unlikely to be explanatory, given that medial temporal sparing persisted when PDD subjects with comparable cognitive impairment were evaluated. Interestingly, amyloid deposition explained the full extent of cortical thinning detected in PD-impaired subjects: cortical thinning was not observed in PD-impaired participants with low amyloid burden. This result builds on previous studies of PDD (Compta et al., 2012; Mak et al., 2017), where CSF markers of AD pathology have been found to correlate with gray matter atrophy and where AD co-pathology at autopsy has been associated with more severe and more widely distributed cortical atrophy (de la Monte et al., 1989).

In contrast to DLB and PD-impaired participants, amyloid deposition did not influence cortical thickness in cognitively normal PD participants. This result suggests that amyloid alone is not responsible for thinning and cognitive impairment, but instead works in concert with other molecular pathologies, including but not limited to neuromodulator loss (Gomperts, 2014; Halliday et al., 2014), cortical alpha-synuclein aggregates (Calo et al., 2016; Colom-Cadena et al., 2017; Schulz-Schaeffer, 2010), and tau deposits (Gomperts et al., 2016; Hansen et al., 2017) that are necessary for the neuropathological cascades that underlie atrophy and accelerate cognitive impairment (Gomperts et al., 2013; Siderowf et al., 2010) in the LBD. In this regard, neurofibrillary tangles measured with tau PET have been shown to correlate with cognitive impairment (Gomperts et al., 2016; Smith et al., 2018).

With respect to the clinical repercussions of cortical thinning, consistent with previous studies (Elder et al., 2017; Sanchez-Castaneda et al., 2009), we observed a strong association in DLB between greater cortical thinning in AD signature regions and greater cognitive functional impairment. Although we found only a trend-level relation in PD-impaired subjects, we anticipate that differences in the extent of cortical thinning and in the severity of cognitive impairment in the DLB and PD-impaired groups may have contributed to this apparent distinction. Similar findings were found for the fusiform region implicated in higher order visual processing (Duchaine and Yovel, 2015), where greater thinning was associated with greater cognitive impairment in DLB. Together, these results suggest that thinning in both AD signature regions and the fusiform cortex contribute to cognitive impairment in the LBD.

In contrast to the impact of regional cortical thinning on cognitive function, we did not detect a significant association between the extent of precentral and paracentral cortical thinning and the severity of motor impairment in any Lewy body disease group. After stratification on the basis of amyloid status, however, such a relationship was evident in amyloid-negative DLB subjects. Due to limited sample sizes in amyloid-stratified subgroups, we consider this result exploratory, but we note that it supports the possibility that the disparate molecular cascades that contribute to cortical thinning in the LBD (synuclein-dependent and amyloid-dependent cascades differentially manifesting in synapse loss, cell death of distinct populations, or other causes of loss of neuropil) may have distinct repercussions on clinical function.

Strengths of this study include the inclusion of clinically well-characterized participants with both DLB and PD across a range of cognitive impairment, including PD-MCI and PDD. The use of Freesurfer permitted high resolution cortical thickness measurements that build on prior volume based approaches. In addition, the stratification of cortical thickness on the basis of amyloid burden has, to our knowledge, never been applied to PD or to its contrast with DLB. However, there are also some limitations. Because healthy control subjects did not undergo amyloid imaging, some controls were likely amyloid positive. This may have reduced our sensitivity to detect differences between the diagnostic groups and the healthy controls. In support of the high specificity of the clinical criteria used to diagnose Lewy body disease, as shown previously (Huang and Halliday, 2013; Nelson et al., 2010), all 18 LBD subjects who underwent neuropathologic assessment had Lewy body disease. In addition, the greater cognitive and motor impairments of the DLB group compared to the PD-impaired group may have contributed to the apparent differences between these groups. However, analyses restricted to PDD subjects gave similar results to those of the PD-impaired group. The diagnostic groups were well-matched for age, and the results of the vertex-based analyses were unchanged after tight matching for age across the groups. Even so, future vertex-wide analyses with larger datasets using age as a covariate will be useful to exclude the possible contribution of group differences in age-related atrophy. Another possible weakness is the small sample sizes of subgroups stratified by amyloid, but the impact of amyloid on cortical thinning was evident in any case. We conclude that the topography of cortical thinning is broadly similar in DLB and PD-associated impairment, is markedly influenced by amyloid deposition, and impacts cognitive function.

CRediT authorship contribution statement

Rong Ye: Data curation, Formal analysis, Investigation, Methodology, Project administration, Software, Validation, Visualization, Writing - original draft, Writing - review & editing. **Alexandra Touroutoglou:** Formal analysis, Investigation, Methodology, Project administration, Software, Validation, Visualization, Writing - original draft, Writing - review & editing. **Michael Brickhouse:** Data curation, Methodology, Project administration, Software, Validation, Visualization. **Samantha Katz:** Data curation, Methodology, Project administration, Software, Validation, Visualization. **John H. Growdon:** Writing - review & editing. **Keith A. Johnson:** Methodology, Resources, Software. **Bradford C. Dickerson:** Conceptualization, Funding acquisition, Investigation, Methodology, Resources, Supervision, Writing - original draft, Writing - review & editing. **Stephen N. Gomperts:** Conceptualization, Funding acquisition, Investigation, Methodology, Resources, Supervision, Writing - original draft, Writing - review & editing.

Declaration of Competing Interest

Dr.. Rong Ye reports no disclosures.

Dr.. Alexandra Touroutoglou reports no disclosures.

Mr. Michael Brickhouse reports no disclosures.

Ms. Samantha Katz reports no disclosures.

Dr.. John Growdon reports support from NIA and Advisory Board Neuroimmune Holding.

Dr.. Keith A. Johnson has served as a paid consultant for Bayer, GE Healthcare, Janssen Alzheimer's Immunotherapy, Siemens Medical Solutions, Genzyme, Novartis, Biogen, Roche, ISIS Pharma, AZTherapy, GEHC, Lundberg, and Abbvie. He is a site coinvestigator for Lilly/Avid, Pfizer, Janssen Immunotherapy, and Navidea. He has spoken at symposia sponsored by Janssen Alzheimer's Immunotherapy and Pfizer. He receives funding from NIH grants R01EB014894, R21 AG038994, R01 AG026484, R01 AG034556, P50 AG00513421, U19 AG10483, P01 AG036694, R13 AG042201174210, R01 AG027435, and R01

AG037497 and the Alzheimer's Association grant ZEN-10–174,210.

Dr.. Bradford C. Dickerson has served as a paid consultant for Novartis, Avexis, Biogen, Lilly, Wave LifeSciences, Merck, and Arkuda. He receives royalties from Oxford University Press and Cambridge University Press. He receives funding from NIH grants P01 AG036694, R01 AG045390, R01 AG038791, R01 AG048351, R01 DC014296, U01 AG052943, R01 AG056015, R21 AG056958, R01 AG054081, R01MH112737, R01MH109464, R01MH113234, R56AG058745, U01AG057195, R01 AG0061968, P01 AG031720, P30AG062421 and the Alzheimer's Drug Discovery Foundation and the ALS Association.

Dr.. Stephen N. Gomperts has served on Advisory Boards for Acadia Pharmaceuticals and Sanofi. He receives funding from NIH grant R01 AG054551, R01 AG062208, P50 AG005134, R21 NS109833, DOD CDMRP/W81XW1810516, the Farmer Family Parkinson's Initiative, and the Lewy Body Dementia Association.

Acknowledgements

The authors thank Larissa Werneck (MGH, Department of Neurology) for research assistance. Research reported in this publication was supported by the Department of Defense CDMRP/W81XW1810516 and the Lewy Body Dementia Association and NIH grant P30AG062421.

Supplementary materials

Supplementary material associated with this article can be found, in the online version, at doi:10.1016/j.nicl.2020.102196.

References

Bakkour, A., Morris, J.C., Dickerson, B.C., 2009. The cortical signature of prodromal AD: regional thinning predicts mild AD dementia. Neurology 72, 1048–1055.

Bakkour, A., Morris, J.C., Wolk, D.A., Dickerson, B.C., 2013. The effects of aging and Alzheimer's disease on cerebral cortical anatomy: specificity and differential relationships with cognition. Neuroimage 76, 332–344.

Beekly, D.L., Ramos, E.M., Lee, W.W., Deitrich, W.D., Jacka, M.E., Wu, J., Hubbard, J.L., Koepsell, T.D., Morris, J.C., Kukull, W.A., Centers, N.I.A.A.s.D., 2007. The national Alzheimer's coordinating center (NACC) database: the uniform data set. Alzheimer Dis Assoc Disord 21, 249–258.

Beyer, M.K., Larsen, J.P., Aarsland, D., 2007. Gray matter atrophy in parkinson disease with dementia and dementia with Lewy bodies. Neurology 69, 747–754.

Bickart, K.C., Brickhouse, M., Negreira, A., Sapolsky, D., Barrett, L.F., Dickerson, B.C., 2014. Atrophy in distinct corticolimbic networks in frontotemporal dementia relates to social impairments measured using the social impairment rating scale. J Neurol Neurosurg Psychiatry 85, 438–448.

Borroni, B., Premi, E., Formenti, A., Turrone, R., Alberici, A., Cottini, E., Rizzetti, C., Gasparotti, R., Padovani, A., 2015. Structural and functional imaging study in dementia with Lewy bodies and Parkinson's disease dementia. Parkinsonism Relat Disord 21, 1049–1055.

Burton, E.J., McKeith, I.G., Burn, D.J., Williams, E.D., O'Brien, J.T., 2004. Cerebral atrophy in Parkinson's disease with and without dementia: a comparison with Alzheimer's disease, dementia with Lewy bodies and controls. Brain 127, 791–800.

Calo, L., Wegrzynowicz, M., Santivanez-Perez, J., Grazia Spillantini, M., 2016. Synaptic failure and alpha-synuclein. Mov Disord 31, 169–177.

Colom-Cadena, M., Pegueroles, J., Herrmann, A.G., Henstridge, C.M., Munoz, L., Querol-Vilaseca, M., Martin-Paniello, C.S., Luque-Cabecerans, J., Clarimon, J., Belbin, O., Nunez-Llaves, R., Blesa, R., Smith, C., McKenzie, C.A., Frosch, M.P., Roe, A., Fortea, J., Andilla, J., Loza-Alvarez, P., Gelpi, E., Hyman, B.T., Spires-Jones, T.L., Lleo, A., 2017. Synaptic phosphorylated alpha-synuclein in dementia with Lewy bodies. Brain 140, 3204–3214.

Compta, Y., Ibarretxe-Bilbao, N., Pereira, J.B., Junque, C., Bargallo, N., Tolosa, E., Valldeoriola, F., Munoz, E., Camara, A., Buongiorno, M., Marti, M.J., 2012. Grey matter volume correlates of cerebrospinal markers of Alzheimer-pathology in Parkinson's disease and related dementia. Parkinsonism Relat Disord 18, 941–947.

de la Monte, S.M., Wells, S.E., Hedley-Whyte, T., Growdon, J.H., 1989. Neuropathological distinction between Parkinson's dementia and Parkinson's plus Alzheimer's disease. Ann Neurol 26, 309–320.

Desikan, R.S., Segonne, F., Fischl, B., Quinn, B.T., Dickerson, B.C., Blacker, D., Buckner, R.L., Dale, A.M., Maguire, R.P., Hyman, B.T., Albert, M.S., Killiany, R.J., 2006. An automated labeling system for subdividing the human cerebral cortex on MRI scans into gyral based regions of interest. Neuroimage 31, 968–980.

Dickerson, B.C., Bakkour, A., Salat, D.H., Feczko, E., Pacheco, J., Greve, D.N., Grodstein, F., Wright, C.I., Blacker, D., Rosas, H.D., Sperling, R.A., Atri, A., Growdon, J.H., Hyman, B.T., Morris, J.C., Fischl, B., Buckner, R.L., 2009. The cortical signature of Alzheimer's disease: regionally specific cortical thinning relates to symptom severity in very mild to mild AD dementia and is detectable in asymptomatic amyloid-positive individuals. Cereb Cortex 19, 497–510.

Dickerson, B.C., Stoub, T.R., Shah, R.C., Sperling, R.A., Killiany, R.J., Albert, M.S., Hyman, B.T., Blacker, D., Detoledo-Morrell, L., 2011. Alzheimer-signature MRI biomarker predicts AD dementia in cognitively normal adults. Neurology 76, 1395–1402.

Duchaine, B., Yovel, G., 2015. A revised neural framework for face processing. Annu Rev Vis Sci 1, 393–416.

Elder, G.J., Mactier, K., Colloby, S.J., Watson, R., Blamire, A.M., O'Brien, J.T., Taylor, J.P., 2017. The influence of hippocampal atrophy on the cognitive phenotype of dementia with Lewy bodies. Int J Geriatr Psychiatry 32, 1182–1189.

Emre, M., Aarsland, D., Brown, R., Burn, D.J., Duyckaerts, C., Mizuno, Y., Broe, G.A., Cummings, J., Dickson, D.W., Gauthier, S., Goldman, J., Goetz, C., Korczyn, A., Lees, A., Levy, R., Litvan, I., McKeith, I., Olanow, W., Poewe, W., Quinn, N., Sampaio, C., Tolosa, E., Dubois, B., 2007. Clinical diagnostic criteria for dementia associated with Parkinson's disease. Mov Disord 22, 1689–1707 quiz 1837.

Ferman, T.J., Smith, G.E., Boeve, B.F., Ivnik, R.J., Petersen, R.C., Knopman, D., Graff-Radford, N., Parisi, J., Dickson, D.W., 2004. DLB fluctuations: specific features that reliably differentiate DLB from AD and normal aging. Neurology 62, 181–187.

Fischl, B., Dale, A.M., 2000. Measuring the thickness of the human cerebral cortex from magnetic resonance images. Proc Natl Acad Sci U S A 97, 11050–11055.

Fischl, B., Sereno, M.I., Dale, A.M., 1999. Cortical surface-based analysis. II: inflation, flattening, and a surface-based coordinate system. Neuroimage 9, 195–207.

Gomperts, S.N., 2014. Imaging the role of amyloid in PD dementia and dementia with Lewy bodies. Curr Neurol Neurosci Rep 14, 472.

Gomperts, S.N., Locascio, J.J., Makaretz, S.J., Schultz, A., Caso, C., Vasdev, N., Sperling, R., Growdon, J.H., Dickerson, B.C., Johnson, K., 2016. Tau positron emission tomographic imaging in the Lewy body diseases. JAMA Neurol 73, 1334–1341.

Gomperts, S.N., Locascio, J.J., Rentz, D., Santarlasci, A., Marquie, M., Johnson, K.A., Growdon, J.H., 2013. Amyloid is linked to cognitive decline in patients with Parkinson disease without dementia. Neurology 80, 85–91.

Greve, D.N., Salat, D.H., Bowen, S.L., Izquierdo-Garcia, D., Schultz, A.P., Catana, C., Becker, J.A., Svarer, C., Knudsen, G.M., Sperling, R.A., Johnson, K.A., 2016. Different partial volume correction methods lead to different conclusions: an (18)F-FDG-PET study of aging. Neuroimage 132, 334–343.

Halliday, G.M., Leverenz, J.B., Schneider, J.S., Adler, C.H., 2014. The neurobiological basis of cognitive impairment in Parkinson's disease. Mov Disord 29, 634–650.

Hansen, A.K., Damholdt, M.F., Fedorova, T.D., Knudsen, K., Parbo, P., Ismail, R., Ostergaard, K., Brooks, D.J., Borghammer, P., 2017. In vivo cortical tau in Parkinson's disease using 18F-AV-1451 positron emission tomography. Mov Disord 32, 922–927.

Harding, A.J., Halliday, G.M., 2001. Cortical Lewy body pathology in the diagnosis of dementia. Acta Neuropathol 102, 355–363.

Harper, L., Bouwman, F., Burton, E.J., Barkhof, F., Scheltens, P., O'Brien, J.T., Fox, N.C., Ridgway, G.R., Schott, J.M., 2017. Patterns of atrophy in pathologically confirmed dementias: a voxelwise analysis. J Neurol Neurosurg Psychiatry 88, 908–916.

Huang, Y., Halliday, G., 2013. Can we clinically diagnose dementia with Lewy bodies yet? Transl Neurodegener 2, 4.

Hughes, A.J., Daniel, S.E., Blankson, S., Lees, A.J., 1993. A clinicopathologic study of 100 cases of Parkinson's disease. Arch Neurol 50, 140–148.

Hyman, B.T., Phelps, C.H., Beach, T.G., Bigio, E.H., Cairns, N.J., Carrillo, M.C., Dickson, D.W., Duyckaerts, C., Frosch, M.P., Masliah, E., Mirra, S.S., Nelson, P.T., Schneider, J.A., Thal, D.R., Thies, B., Trojanowski, J.Q., Vinters, H.V., Montine, T.J., 2012. National institute on aging-alzheimer's association guidelines for the neuropathologic assessment of Alzheimer's disease. Alzheimers Dement 8, 1–13.

Kang, S.W., Jeon, S., Yoo, H.S., Chung, S.J., Lee, P.H., Sohn, Y.H., Yun, M., Evans, A.C., Ye, B.S., 2019. Effects of Lewy body disease and Alzheimer disease on brain atrophy and cognitive dysfunction. Neurology 92, e2015–e2026.

Kuperberg, G.R., Broome, M.R., McGuire, P.K., David, A.S., Eddy, M., Ozawa, F., Goff, D., West, W.C., Williams, S.C., van der Kouwe, A.J., Salat, D.H., Dale, A.M., Fischl, B., 2003. Regionally localized thinning of the cerebral cortex in schizophrenia. Arch Gen Psychiatry 60, 878–888.

Lee, J.E., Park, B., Song, S.K., Sohn, Y.H., Park, H.J., Lee, P.H., 2010. A comparison of gray and white matter density in patients with Parkinson's disease dementia and dementia with Lewy bodies using voxel-based morphometry. Mov Disord 25, 28–34.

Lee, Y.G., Jeon, S., Yoo, H.S., Chung, S.J., Lee, S.K., Lee, P.H., Sohn, Y.H., Yun, M., Evans, A.C., Ye, B.S., 2018. Amyloid-beta-related and unrelated cortical thinning in dementia with Lewy bodies. Neurobiol Aging 72, 32–39.

Litvan, I., Goldman, J.G., Troster, A.I., Schmand, B.A., Weintraub, D., Petersen, R.C., Mollenhauer, B., Adler, C.H., Marder, K., Williams-Gray, C.H., Aarsland, D., Kulisevsky, J., Rodriguez-Oroz, M.C., Burn, D.J., Barker, R.A., Emre, M., 2012. Diagnostic criteria for mild cognitive impairment in Parkinson's disease: movement disorder society task force guidelines. Mov Disord 27, 349–356.

Mak, E., Donaghy, P.C., McKiernan, E., Firbank, M.J., Lloyd, J., Petrides, G.S., Thomas, A.J., O'Brien, J.T., 2019. Beta amyloid deposition maps onto hippocampal and subiculum atrophy in dementia with Lewy bodies. Neurobiol Aging 73, 74–81.

Mak, E., Su, L., Williams, G.B., Firbank, M.J., Lawson, R.A., Yarnall, A.J., Duncan, G.W., Mollenhauer, B., Owen, A.M., Khoo, T.K., Brooks, D.J., Rowe, J.B., Barker, R.A., Burn, D.J., O'Brien, J.T., 2017. Longitudinal whole-brain atrophy and ventricular enlargement in nondemented Parkinson's disease. Neurobiol Aging 55, 78–90.

McKeith, I.G., Boeve, B.F., Dickson, D.W., Halliday, G., Taylor, J.P., Weintraub, D., Aarsland, D., Galvin, J., Attems, J., Ballard, C.G., Bayston, A., Beach, T.G., Blanc, F., Bohnen, N., Bonanni, L., Bras, J., Brundin, P., Burn, D., Chen-Plotkin, A., Duda, J.E., El-Agnaf, O., Feldman, H., Ferman, T.J., Ffytche, D., Fujishiro, H., Galasko, D., Goldman, J.G., Gomperts, S.N., Graff-Radford, N.R., Honig, L.S., Iranzo, A., Kantarci, K., Kaufer, D., Kukull, W., Lee, V.M.Y., Leverenz, J.B., Lewis, S., Lippa, C., Lunde, A., Masellis, M., Masliah, E., McLean, P., Mollenhauer, B., Montine, T.J., Moreno, E.,

Mori, E., Murray, M., O'Brien, J.T., Orimo, S., Postuma, R.B., Ramaswamy, S., Ross, O.A., Salmon, D.P., Singleton, A., Taylor, A., Thomas, A., Tiraboschi, P., Toledo, J.B., Trojanowski, J.Q., Tsuang, D., Walker, Z., Yamada, M., Kosaka, K., 2017. Diagnosis and management of dementia with Lewy bodies: fourth consensus report of the DLB consortium. Neurology 89, 88–100.

Moriguchi, Y., Negreira, A., Weierich, M., Dautoff, R., Dickerson, B.C., Wright, C.I., Barrett, L.F., 2011. Differential hemodynamic response in affective circuitry with aging: an FMRI study of novelty, valence, and arousal. J Cogn Neurosci 23, 1027–1041.

Mormino, E.C., Betensky, R.A., Hedden, T., Schultz, A.P., Ward, A., Huijbers, W., Rentz, D.M., Johnson, K.A., Sperling, R.A., Alzheimer's disease neuroimaging, I., australian imaging, B., lifestyle flagship study of, A., harvard aging brain, S., 2014. Amyloid and APOE epsilon4 interact to influence short-term decline in preclinical Alzheimer disease. . Neurology 82, 1760–1767.

Morris, J.C., Weintraub, S., Chui, H.C., Cummings, J., Decarli, C., Ferris, S., Foster, N.L., Galasko, D., Graff-Radford, N., Peskind, E.R., Beekly, D., Ramos, E.M., Kukull, W.A., 2006. The uniform data set (UDS): clinical and cognitive variables and descriptive data from alzheimer disease centers. Alzheimer Dis Assoc Disord 20, 210–216.

Nelson, P.T., Jicha, G.A., Kryscio, R.J., Abner, E.L., Schmitt, F.A., Cooper, G., Xu, L.O., Smith, C.D., Markesbery, W.R., 2010. Low sensitivity in clinical diagnoses of dementia with Lewy bodies. J Neurol 257, 359–366.

Racine, A.M., Brickhouse, M., Wolk, D.A., Dickerson, B.C., Alzheimer's Disease Neuroimaging, I., 2018. The personalized Alzheimer's disease cortical thickness index predicts likely pathology and clinical progression in mild cognitive impairment. Alzheimers Dement (Amst) 10, 301–310.

Rosas, H.D., Liu, A.K., Hersch, S., Glessner, M., Ferrante, R.J., Salat, D.H., van der Kouwe, A., Jenkins, B.G., Dale, A.M., Fischl, B., 2002. Regional and progressive thinning of the cortical ribbon in Huntington's disease. Neurology 58, 695–701.

Salat, D.H., Buckner, R.L., Snyder, A.Z., Greve, D.N., Desikan, R.S., Busa, E., Morris, J.C., Dale, A.M., Fischl, B., 2004. Thinning of the cerebral cortex in aging. Cereb Cortex 14, 721–730.

Sanchez-Castaneda, C., Rene, R., Ramirez-Ruiz, B., Campdelacreu, J., Gascon, J., Falcon, C., Calopa, M., Jauma, S., Juncadella, M., Junque, C., 2009. Correlations between gray matter reductions and cognitive deficits in dementia with Lewy bodies and Parkinson's disease with dementia. Mov Disord 24, 1740–1746.

Sarro, L., Senjem, M.L., Lundt, E.S., Przybelski, S.A., Lesnick, T.G., Graff-Radford, J., Boeve, B.F., Lowe, V.J., Ferman, T.J., Knopman, D.S., Comi, G., Filippi, M., Petersen, R.C., Jack Jr., C.R., Kantarci, K., 2016. Amyloid-beta deposition and regional grey matter atrophy rates in dementia with Lewy bodies. Brain 139, 2740–2750.

Schulz-Schaeffer, W.J., 2010. The synaptic pathology of alpha-synuclein aggregation in dementia with Lewy bodies. Parkinson's disease and Parkinson's disease dementia. Acta Neuropathol 120, 131–143.

Shimada, H., Shinotoh, H., Hirano, S., Miyoshi, M., Sato, K., Tanaka, N., Ota, T., Fukushi, K., Irie, T., Ito, H., Higuchi, M., Kuwabara, S., Suhara, T., 2013. beta-Amyloid in Lewy body disease is related to Alzheimer's disease-like atrophy. Mov Disord 28, 169–175.

Siderowf, A., Xie, S.X., Hurtig, H., Weintraub, D., Duda, J., Chen-Plotkin, A., Shaw, L.M., Van Deerlin, V., Trojanowski, J.Q., Clark, C., 2010. CSF amyloid {beta} 1-42 predicts cognitive decline in parkinson disease. Neurology 75, 1055–1061.

Smith, R., Scholl, M., Londos, E., Ohlsson, T., Hansson, O., 2018. (18)F-AV-1451 in Parkinson's disease with and without dementia and in dementia with Lewy bodies. Sci Rep 8, 4717.

Song, S.K., Lee, J.E., Park, H.J., Sohn, Y.H., Lee, J.D., Lee, P.H., 2011. The pattern of cortical atrophy in patients with Parkinson's disease according to cognitive status. Mov Disord 26, 289–296.

Summerfield, C., Junque, C., Tolosa, E., Salgado-Pineda, P., Gomez-Anson, B., Marti, M.J., Pastor, P., Ramirez-Ruiz, B., Mercader, J., 2005. Structural brain changes in parkinson disease with dementia: a voxel-based morphometry study. Arch Neurol 62, 281–285.

van der Zande, J.J., Steenwijk, M.D., Ten Kate, M., Wattjes, M.P., Scheltens, P., Lemstra, A.W., 2018. Gray matter atrophy in dementia with Lewy bodies with and without concomitant Alzheimer's disease pathology. Neurobiol Aging 71, 171–178.

Watson, R., Colloby, S.J., Blamire, A.M., O'Brien, J.T., 2015. Assessment of regional gray matter loss in dementia with Lewy bodies: a surface-based MRI analysis. Am J Geriatr Psychiatry 23, 38–46.

Weintraub, D., Doshi, J., Koka, D., Davatzikos, C., Siderowf, A.D., Duda, J.E., Wolk, D.A., Moberg, P.J., Xie, S.X., Clark, C.M., 2011. Neurodegeneration across stages of cognitive decline in parkinson disease. Arch Neurol 68, 1562–1568.